S1. Challenges for modelling ET and representing land cover properties explicitly at large-scales

Representing explicitly land cover properties for ET estimation requires the specification of vegetation properties, such as leaf area index, vegetation height, stomatal resistance, canopy interception storage capacity, and the availability of time series of climate variables such as air temperature, net radiation, humidity and wind speed. Modelling ET at large-scales faces a range of challenges: (1) a lack of ET observations to compare with model simulations, (2) a lack of observations of vegetation properties, and (3) uncertainty in large-scale forcing weather variables.

Firstly, on the ground, measurements of actual ET (e.g. FLUXNET network (Baldocchi et al., 2001)) are limited in number and are only representative of plot scale ET. Their footprint can extend to a few hundred metres or possibly to a few kilometres (Baldocchi and Ryu, 2011), which is much smaller than the extent of typical large-scale model simulation units that are mostly between 9 km (5' grid) and 111 km (1° grid) (Bierkens, 2016). Moreover, ground measurements of the partitioning of ET among its main components (transpiration, evaporation from interception and soil evaporation) are lacking as reported in (Miralles et al., 2016), and the ET partitioning assessed using isotope techniques has large uncertainties and limited spatial coverage (Coenders-Gerrits et al., 2014; Sutanto et al., 2014). Additionally, global gridded ET products are available. Yet, these products do not provide direct observations of actual ET, but they are estimates of actual ET assessed using models that assimilate remote-sensed variables and either solve the energy balance or use potential ET (PET) equations as discussed in e.g. (McCabe et al., 2016; Miralles et al., 2016). Additionally, (Jung et al., 2011) created a global gridded ET products based on model tree ensembles which are trained using observations from the FLUXNET network.

A second issue is that observations of large-scale vegetation properties are limited. Large-scale gridded land cover databases provide spatially distributed information about the type of vegetation present around the world. We refer to (Smith, 2016) for a review of land cover databases. However, large-scale gridded measurements of vegetation characteristics are obtained using remote-sensing techniques and are restricted to optical properties. Remote sensing techniques permit to retrieve vegetation leaf area index (LAI) (see e.g. (Fang et al., 2013)) and other vegetation indices that can be only used as proxy for actual vegetation properties such as density or state of health, for instance Vegetation Optical Depth (VOD), Normalized Difference Vegetation Index (NDVI) or Enhanced Vegetation Index (EVI) (see a review in (Xue and Su, 2017)). Moreover, such products suffer from a number of uncertainties, among which cloud contamination as reported for instance in (Fang et al., 2013) regarding LAI, and do not allow to assess critical vegetation properties such as rooting depth, stomatal resistance or canopy interception capacity. Ground measurements of vegetation properties are sparse and only few studies report collected values for specific variables or regions, these include (Breuer et al., 2003) for a range of vegetation properties in temperate climates, (Körner, 1995) for stomatal resistance and (Schenk and Jackson, 2002) for rooting depth. Since ground measurements are limited, they do not allow to capture the variability in vegetation characteristics, as discussed in (Wang-Erlandsson et al., 2016) regarding rooting depth measurements. In particular, stomatal resistance presents a high temporal variability because it is determined by weather conditions and therefore its measurements are particularly difficult to interpret (Breuer et al., 2003) and to use in modelling applications.

Thirdly, large-scale databases of historical weather data used to force model simulations are affected by large uncertainties because they have to rely on measurements with incomplete spatial coverage, in particular wind speed measurements (New et al., 2002). Moreover, the height from the ground at which these weather data are provided is uncertain. Measurements are assumed to be provided at standard heights, typically 10 m for wind speed and 2 m for temperature and humidity (see e.g. (Rodell et al., 2004; Weedon et al., 2010)), which may not be representative of the specific location.

S2. Parameters used for ET estimation in large-scale models

Parameter	Description	Module [a]	Category	Unit	Reference
Z_r	Rooting depth	Stress	Vegetation	[m]	(Vörösmarty et al., 1989)
AWC	Soil available water capacity	Stress	Soil	[$m^3.m^{-3}$]	(Vörösmarty et al., 1989)
α	Empirical coefficient of the drying curve (set to 5)	Stress	Constant	[-]	(Vörösmarty et al., 1998)

Table S1. Parameters used for ET estimation in the WBM model. The model includes a minimum of 3 parameters (reported in the table), and additional parameters depending on the PET formulation which is used (namely the Thornthwaite equation (Thornthwaite, 1948) in (Vörösmarty et al., 1996), the Shuttleworth-Wallace (Shuttleworth and Wallace, 1985) equation in (Federer et al., 2003), and a range of different PET equations in (Vörösmarty et al., 1998)).

[a] Stress: Stress model for actual ET calculation

Parameter	Description	Module [a]	Category	Unit	Reference
z_0	Surface roughness length	PET	Vegetation	[m]	(Milly and Shmakin, 2002)
r_s	Bulk stomatal resistance (surface resistance)	PET	Vegetation	[$s.m^{-1}$]	(Milly and Shmakin, 2002)
Z_r	Rooting depth	Stress	Vegetation	[m]	(Milly and Shmakin, 2002)
AWC	Soil available water capacity	Stress	Soil	[$kg.m^{-3}$]	(Milly and Shmakin, 2002)
W_1	Constant in soil moisture stress function (set to 0.75)	Stress	Constant	[-]	(Milly and Shmakin, 2002)

Table S2. Parameters used for ET estimation in the LaD model.

[a] PET: potential evapotranspiration equation; Stress: Stress model for actual ET calculation from PET.

Parameter	Description	Module [a]	Category	Unit	Reference
α_{PT}	Priestley-Taylor empirical coefficient (1.26 in semiarid and arid areas and 1.74 in humid areas)	PET	Climate	[-]	(Döll et al., 2003)
$E_{pot,max}$	Maximum potential evapotranspiration (20 mmd^{-1} in semiarid and arid areas and 10 mmd^{-1} in humid areas)	Stress	Climate	[$mm.d^{-1}$]	(Müller Schmied et al., 2014)
Z_r	Rooting depth	Stress	Vegetation	[m]	(Müller Schmied et al., 2014)
AWC	Soil available water capacity	Stress	Soil	[$m^3.m^{-3}$]	(Döll et al., 2003)
V_{can}	Interception storage capacity per unit of LAI (set to 0.3 mm LAI)	Interception	Constant	[mm LAI]	(Döll et al., 2003)
Exp_{can}	Exponent to assess the wet canopy fraction (set to 2/3)	Interception	Constant	[-]	(Deardorff, 1978; Döll et al., 2003)
LAI_{max}	Maximum leaf area index	Interception	Vegetation	[$m^2.m^{-2}$]	(Müller Schmied et al., 2014)
$f_{d,lc}$	Fraction of deciduous plants in LAI growth model	Seasonality	Vegetation	[-]	(Müller Schmied et al., 2014)
$c_{e,lc}$	Reduction factor for evergreen plants in LAI growth model	Seasonality	Vegetation	[-]	(Müller Schmied et al., 2014)
t_{min}	Initial days to start/end with growing season in LAI growth model	Seasonality	Vegetation	[d]	(Müller Schmied et al., 2014)
LAI_{min}	Minimum leaf area index for deciduous plants in LAI growth model (set to 0.1 $m^2.m^{-2}$)	Seasonality	Constant	[$m^2.m^{-2}$]	(Müller Schmied et al., 2014)
T_{min}	Daily temperature threshold to initiate the growing season in LAI growth model (set to 8°C)	Seasonality	Constant	[°C]	(Müller Schmied et al., 2014)
$P_{min,cum}$	Cumulative precipitation threshold to initiate the growing season in LAI growth model (set to 40mm)	Seasonality	Constant	[mm]	(Müller Schmied et al., 2014)
$P_{min,daily}$	Minimum daily precipitation to keep growing season growing in semi-arid and arid regions in LAI growth model (set to 0.5mm)	Seasonality	Constant	[$mm.d^{-1}$]	(Müller Schmied et al., 2014)
t_{growth}	Number of days for LAI to increase from its minimum to its maximum value or to decrease from its maximum to its minimum value in LAI growth model (set to 30 d)	Seasonality	Constant	[d]	(Müller Schmied et al., 2014)

Table S3. Parameters used for ET estimation in the WaterGap V2.2 model.

[a] PET: potential evapotranspiration equation; Stress: Stress model for actual ET calculation from PET.

Parameter	Description	Module [a]	Category	Unit	Reference
g_{min}	Minimum canopy conductance	PET	Vegetation	[mm.s^{-1}]	(Gerten et al., 2004; Sitch et al., 2003)
g_m	Scaling conductance in the evaporative demand function (set to 3.26 mm.s^{-1})	PET	Constant	[mm.s^{-1}]	(Gerten et al., 2004)
α_m	Priestley-Taylor empirical coefficient (set to 1.391)	PET	Constant	[-]	(Gerten et al., 2004)
α_{PT}	Priestley-Taylor empirical coefficient (set to 1.32)	PET	Constant	[-]	(Gerten et al., 2004)
i	Empirical coefficient for calculation of interception (same formulation as (Kergoat, 1998))	Interception	Vegetation	[-]	(Gerten et al., 2004)
LAI	Leaf area index (determined as a function of daily phenomenology)	Interception	Vegetation	[m^2.m^{-2}]	(Gerten et al., 2004)
$E_{pot,max}$	Maximum potential evapotranspiration (5-7 mm.d^{-1})	Stress	Vegetation	[mm.d^{-1}]	(Gerten et al., 2004)
AWC	Soil available water capacity	Stress	Soil	[m^3.m^{-3}]	(Gerten et al., 2004)
$f_{root,0}$	Weighting constant to determine fraction of roots in evaporation layer (set to 1.3)	Stress	Constant	[-]	(Gerten et al., 2004)
$f_{root,1}$	fraction of roots in soil layer 1	Stress	Vegetation	[-]	(Gerten et al., 2004; Sitch et al., 2003)
d_1	depth soil layer 1 (set to 0.5 m)	Soil layers	Constant	[m]	(Gerten et al., 2004)
d_2	depth soil layer 2 (set to 1 m)	Soil layers	Constant	[m]	(Gerten et al., 2004)
d_0	depth evaporation layer (set to 0.2 m)	Soil layers	Constant	[m]	(Gerten et al., 2004)
f_c	Vegetation cover fraction (determined as a function of daily phenomenology)	Sparse vegetation	Vegetation	[-]	(Gerten et al., 2004)

Table S4. Parameters used for ET estimation in the LPJ model.

[a] PET: potential evapotranspiration equation; Stress: Stress model for actual ET calculation from PET.

Parameter	Description	Module [a]	Category	Unit	Reference
$r_{a,veg}$	Vegetation aerodynamic resistance	PET	Vegetation	[$s.m^{-1}$]	(Kergoat, 1998)
r_{st}	Minimum stomatal resistance	PET	Vegetation	[$s.m^{-1}$]	(Kergoat, 1998)
$r_{a,soi}$	Soil aerodynamic resistance (set to 100 $s.m^{-1}$)	PET	Constant	[$s.m^{-1}$]	(Kergoat, 1998)
$r_{s,soi}$	Soil surface resistance (set to 50 $s.m^{-1}$)	PET	Constant	[$s.m^{-1}$]	(Kergoat, 1998)
LAI	Leaf area index	PET and interception	Vegetation	[$m^2.m^{-2}$]	(Kergoat, 1998)
β	Empirical coefficient for calculation of interception	Interception	Vegetation	[-]	(Kergoat, 1998)
S_1	Constant in radiation term in stomatal resistance parameterization (set to 10 W PAR.$m^{-2)}$	PET (surface resistance)	Constant	[W PAR .m^{-2}]	(Kergoat, 1998)
f_s	Fraction of photosynthetically active solar radiation (set to 0.48)	PET (surface resistance)	Constant	[-]	(Kergoat, 1998)
D_1	First coefficient of the vapour pressure deficit term in stomatal resistance parameterization (set to 3000 Pa)	PET (surface resistance)	Constant	[Pa]	(Kergoat, 1998)
D_2	Second coefficient of the vapour pressure deficit term in stomatal resistance parameterization (set to 3500 Pa)	PET (surface resistance)	Constant	[Pa]	(Kergoat, 1998)
k	Beer- Lambert extinction coefficient (set to 0.5)	PET (surface resistance) and Sparse vegetation	Constant	[-]	(Kergoat, 1998)
Z_r	Rooting depth	Stress	Vegetation	[m]	(Kergoat, 1998)
AWC	Soil available water capacity	Stress	Soil	[$m^3.m^{-3}$]	(Kergoat, 1998)
W_1	Soil water constant for stomatal closure as a fraction of soil water storage (set to 0.4)	Stress	Constant	[-]	(Kergoat, 1998)
W_2	Soil water constant for soil evaporation reduction (set to 0.6)	Stress	Constant	[-]	(Kergoat, 1998)

Table S5. Parameters used for ET estimation in the model proposed by (Kergoat, 1998). We did not review the light limitation sub-model of the model, which is used to calculate an equilibrium value of LAI.

[a] PET: potential evapotranspiration equation; Stress: Stress model for actual ET calculation from PET.

Parameter	Description	Module [a]	Category	Unit	Reference
K_c	Crop factor (monthly values estimated as a function of land cover and climatology)	PET (and seasonality)	Vegetation	[-]	(Van Beek, 2008)
$K_{c,min}$	Minimum crop factor for bare soil (set to 0.2)	PET	Constant	[-]	(Van Beek, 2008; Sperna Weiland et al., 2015)
LAI	Leaf area index (monthly values estimated as a function of land cover and climatology)	Interception (and seasonality)	Vegetation	[$m^2.m^{-2}$]	(Van Beek, 2008; Sutanudjaja et al., 2011)
V_{can}	Interception storage capacity (set to 0.3 mm LAI)	Interception	Constant	[mm LAI]	(Sutanudjaja et al., 2011)
$f_{root,1}$	Root fraction in soil layer 1	Stress	Vegetation	[-]	(Van Beek, 2008; Sperna Weiland et al., 2015; Sutanudjaja et al., 2011)
β_1	Coefficient of the soil water retention curve in soil layer 1	Stress	Soil	[-]	(Van Beek, 2008; Sutanudjaja et al., 2011)
β_2	Coefficient of the soil water retention curve in soil layer 2	Stress	Soil	[-]	(Van Beek, 2008; Sutanudjaja et al., 2011)
$W_{sat,1}$	Saturated volumetric moisture content in soil layer 1	Stress	Soil	[$m^3.m^{-3}$]	(Van Beek and Bierkens, 2008; Sperna Weiland et al., 2015)
$W_{sat,2}$	Saturated volumetric moisture content in soil layer 2	Stress	Soil	[$m^3.m^{-3}$]	(Van Beek and Bierkens, 2008; Sperna Weiland et al., 2015)
$k_{sat,1}$	Saturated hydraulic conductivity in soil layer 1	Stress (soil evaporation)	Soil	[$m.d^{-1}$]	(Van Beek, 2008; Sutanudjaja et al., 2011)
$\Psi_{sat,1}$	Matric soil suction at saturation in soil layer 1	Stress (transpiration)	Soil	[m]	(Sutanudjaja et al., 2011)
$\Psi_{sat,2}$	Matric soil suction at saturation in soil layer 2	Stress (transpiration)	Soil	[m]	(Sutanudjaja et al., 2011)
$\Psi_{50\%}$	Matric soil suction at which transpiration is halved (set for instance equal to 3.33m)	Stress (transpiration)	Constant	[m]	(Sutanudjaja et al., 2011)
d_1	Depth of soil layer 1 (set to 0.3 m)	Stress	Constant	[m]	(Van Beek and Bierkens, 2008)
d_2	Depth of soil layer 2 (set to 1.2 m)	Stress	Constant	[m]	(Van Beek and Bierkens, 2008)

Table S6. Parameters used for ET estimation in the PCR-GLOBWB model.

[a] PET: potential evapotranspiration equation; Stress: Stress model for actual ET calculation from PET.

Parameter	Description	Module [a]	Category	Unit	Reference
$h_{veg,over}$	Overstory vegetation height	PET	Overstory vegetation	[m]	(Gosling and Arnell, 2011; Smith, 2016)
$r_{st,over}$	Overstory vegetation stomatal resistance	PET	Overstory vegetation	[s.m^{-1}]	(Gosling and Arnell, 2011; Smith, 2016)
LAI_{over}	Overstory leaf area index	PET	Overstory vegetation	[m^2.m^{-2}]	(Gosling and Arnell, 2011; Smith, 2016)
$h_{veg,over}$	Understory vegetation height (set to value for grass)	PET	Understory vegetation	[m]	(Gosling and Arnell, 2011; Smith, 2016)
$r_{st,under}$	Understory vegetation stomatal resistance (set to value for grass)	PET	Understory vegetation	[s.m^{-1}]	(Gosling and Arnell, 2011; Smith, 2016)
LAI_{under}	Understory leaf area index (set to value for grass)	PET	Understory vegetation	[m^2.m^{-2}]	(Gosling and Arnell, 2011; Smith, 2016)
K	Radiation coefficient to calculate canopy surface resistance (set to 0.7)	PET	Constant	[-]	(Smith, 2016)
$r_{s,soi}$	(Soil) resistance to calculate canopy surface resistance (set to 100 s.m^{-1})	PET	Constant	[s.m^{-1}]	(Smith, 2016)
$Z_{r,over}$	Overstory rooting depth	Stress	Overstory vegetation	[m]	(Gosling and Arnell, 2011; Smith, 2016)
$Z_{r,under}$	Understory rooting depth (set to value for grass)	Stress	Understory vegetation	[m]	(Gosling and Arnell, 2011; Smith, 2016)
FC	Soil field capacity	Stress	Soil	[m^3.m^{-3}]	(Gosling and Arnell, 2011; Smith, 2016)
S_{max}	Soil saturation capacity	Stress	Soil	[m^3.m^{-3}]	(Gosling and Arnell, 2011; Smith, 2016)
γ_{over}	Overstory interception capacity	Interception	Overstory vegetation	[mm]	(Gosling and Arnell, 2011; Smith, 2016)
γ_{under}	Understory interception capacity (set to value for grass)	Interception	Understory vegetation	[mm]	(Gosling and Arnell, 2011; Smith, 2016)
δ	Empirical parameter of interception model (set to 0.75)	Interception	Constant	[-]	(Arnell, 1999; Smith, 2016)
$Percov$	Percent overstory cover	Sparse vegetation	Overstory vegetation	[%]	(Gosling and Arnell, 2011; Smith, 2016)

Table S7. Parameters used for ET estimation in the Mac-PDM model.

[a] PET: potential evapotranspiration equation; Stress: Stress model for actual ET calculation from PET.

Parameter	Description	Module [a]	Category	Unit	Reference
z_0	Surface roughness length	PET	Vegetation	[m]	(Noilhan and Planton, 1989)
r_{st}	Minimum stomatal resistance	PET	Vegetation	[$s.m^{-1}$]	(Noilhan and Planton, 1989)
LAI	Leaf area index (average monthly values)	PET and interception	Vegetation	[$m^2.m^{-2}$]	(Noilhan and Planton, 1989)
V_{can}	Interception storage capacity per unit of LAI (set to 0.2 mm LAI)	Interception	Constant	[mm LAI]	(Noilhan and Planton, 1989)
Exp_{can}	Exponent to assess the wet canopy fraction (set to 2/3)	Interception	Constant	[-]	(Deardorff, 1978; Noilhan and Planton, 1989)
R_{GL}	Limit value of incoming solar radiation (set to 30 W m^{-2} for forest and 100 W m^{-2} for crop)	PET (surface resistance)	Vegetation	[W m^{-2}]	(Noilhan and Planton, 1989)
$r_{st,max}$	Maximum surface resistance (set to 5000 $s.m^{-1}$)	PET (surface resistance)	Constant	[$s.m^{-1}$]	(Noilhan and Planton, 1989)
f_s	Fraction of photosynthetically active solar radiation (set to 0.55)	PET (surface resistance)	Constant	[-]	(Noilhan and Planton, 1989)
g	Coefficient of the vapour pressure term (set to 0.025 hPa^{-1})	PET (surface resistance)	Constant	[hPa^{-1}]	(Noilhan and Planton, 1989)
k_T	Coefficient of the temperature term (set to 0.0016 K^{-2})	PET (surface resistance)	Constant	[K^{-2}]	(Noilhan and Planton, 1989)
WP	Wilting point volumetric water content	Stress	Soil	[$m^3.m^{-3}$]	(Noilhan and Planton, 1989)
W_{sat}	Saturated volumetric moisture content	Stress	Soil	[$m^3.m^{-3}$]	(Noilhan and Planton, 1989)
W_{crit}	Critical soil moisture (set to 0.75)	Stress	Constant	[-]	(Noilhan and Planton, 1989)
d_1	Depth of the evaporation soil layer (set to 0.01m))	Stress	Constant	[m]	(Noilhan and Planton, 1989)
d_2	Rooting depth	Stress	Vegetation	[m]	(Noilhan and Planton, 1989)
d_3	Total soil depth	Stress	Vegetation and soil	[m]	(Boone et al., 1999)
f_c	Vegetation cover fraction	Sparse vegetation	Vegetation	[-]	(Noilhan and Planton, 1989)

Table S8. Parameters used for ET estimation in the ISBA model.

[a] PET: potential evapotranspiration equation; Stress: Stress model for actual ET calculation from PET.

Parameter	Description	Module [a]	Category	Unit	Reference
α_{PT}	Priestley-Taylor empirical coefficient	PET	Vegetation	[-]	(Miralles et al., 2011)
f_G	Ground heat as a fraction of net radiation	PET	Vegetation	[-]	(Miralles et al., 2011)
β	Correction factor for transpiration to account for hours with wet canopy (set to 0.07)	PET (tall vegetation)	Constant	[-]	(Miralles et al., 2011)
VOD	Vegetation optical depth (remotely sensed)	Stress and seasonality	Vegetation	[-]	(Martens et al., 2017; Miralles et al., 2011)
VOD_{max}	Maximum vegetation optical depth	Stress	Vegetation	[-]	(Martens et al., 2017)
Z_r	Rooting depth	Stress	Vegetation	[m]	(Miralles et al., 2011)
WP	Wilting point	Stress	Soil	[$m^3.m^{-3}$]	(Martens et al., 2017)
FC	Field capacity	Stress	Soil	[$m^3.m^{-3}$]	(Martens et al., 2017)
S_c	Canopy storage for tall vegetation (set to 1.2 mm)	Interception (tall vegetation)	Constant	[mm]	(Miralles et al., 2010)
$\overline{E_c}$	Mean evaporation rate for interception for tall vegetation (set to 0.3 $mm.h^{-1}$)	Interception (tall vegetation)	Constant	[$mm.h^{-1}$]	(Miralles et al., 2010)
$\overline{R_s}$	Mean (synoptic) rainfall rate for tall vegetation (set to 1.5 $mm.h^{-1}$)	Interception (tall vegetation)	Constant	[$mm.h^{-1}$]	(Miralles et al., 2010)
$\overline{R_c}$	Mean (convective) rainfall rate for tall vegetation (set to 5.6 $mm.h^{-1}$)	Interception (tall vegetation)	Constant**)**	[$mm.h^{-1}$]	(Miralles et al., 2010)
p_d	Fraction of rain to trunks for tall vegetation (set to 0.02)	Interception (tall vegetation)	Constant	[-]	(Miralles et al., 2010)
e	Fraction of trunk evaporation for tall vegetation (set to 0.02)	Interception (tall vegetation)	Constant	[-]	(Miralles et al., 2010)
S_t	Trunk capacity for tall vegetation (set to 0.02 mm)	Interception (tall vegetation)	Constant	[mm]	(Miralles et al., 2010)
d_1	Depth at the bottom of the first soil layer (set to 0.05m)	Soil layers	Constant	[m]	(Miralles et al., 2011)
d_2	Depth at the bottom of the second soil layer (set to 1 m)	Soil layers	Constant	[m]	(Miralles et al., 2011)
d_3	Depth at the bottom of the third soil layer (set to 2.5 m)	Soil layers	Constant	[m]	(Miralles et al., 2011)

Table S9. Parameters used for ET estimation in the GLEAM V3 model.

[a] PET: potential evapotranspiration equation; Stress model for actual ET calculation from PET.

Parameter	Description	Module [a]	Category	Unit	Reference
z_0	Surface roughness length	PET	Vegetation	[m]	(Liang et al., 1994)
r_{st}	Minimum stomatal resistance	PET	Vegetation	[s.m^{-1}]	(Bohn and Vivoni, 2016; Liang et al., 1994)
r_{arc}	Vegetation architectural resistance (boundary layer resistance)	PET	Vegetation	[s.m^{-1}]	(Bohn and Vivoni, 2016; Liang et al., 1994)
d_0	Vegetation zero plane displacement height	PET	Vegetation	[m]	(Liang et al., 1994)
$r_{s,soi}$	Soil surface resistance (set to 0 s.m^{-1})	PET	Constant	[s.m^{-1}]	(Bohn and Vivoni, 2016)
$r_{arc,soi}$	Soil architectural resistance (set to 0 s.m^{-1})	PET	Constant	[s.m^{-1}]	(Bohn and Vivoni, 2016)
LAI	Leaf area index (average monthly values)	PET and interception	Vegetation	[m^2.m^{-2}]	(Bohn and Vivoni, 2016; Liang et al., 1994)
V_{can}	Interception storage capacity per unit of LAI (set to 0.2 mm LAI)	Interception	Constant	[mm LAI]	(Liang et al., 1994)
Exp_{can}	Exponent to assess the wet canopy fraction (set to 2/3)	Interception	Constant	[-]	(Deardorff, 1978; Liang et al., 1994)
R_{GL}	Limit value of incoming solar radiation	PET (surface resistance)	Vegetation	[W m^{-2}]	(Bohn and Vivoni, 2016)
$r_{st,max}$	Maximum surface resistance	PET (surface resistance)	Constant	[s.m^{-1}]	(Bohn and Vivoni, 2016)
f_s	Fraction of photosynthetically active solar radiation	PET (surface resistance)	Constant	[-]	(Bohn and Vivoni, 2016)
g	Coefficient of the vapour pressure deficit term	PET (surface resistance)	Constant	[hPa^{-1}]	(Bohn and Vivoni, 2016)
k_T	Coefficient of the temperature term	PET (surface resistance)	Constant	[K^{-2}]	(Bohn and Vivoni, 2016)
$f_{root,1}$	Root fraction in first soil layer	Stress	Vegetation	[-]	(Liang et al., 1994)
W_{crit}	Critical soil moisture in stomatal resistance parameterization as a fraction of soil saturation	Stress	Soil	[m^3.m^{-3}]	(Bohn and Vivoni, 2016; Liang et al., 1994)
WP	Wilting point	Stress	Soil	[m^3.m^{-3}]	(Bohn and Vivoni, 2016; Liang et al., 1994)
d_1	Depth of soil layer 1 (e.g. set to 0.3 m)	Stress	Constant	[m]	(Liang et al., 1994)
d_2	Depth of soil layer 2 (e.g. set to 0.7 m)	Stress	Constant	[m]	(Liang et al., 1994)
$NDVI$	Normalized Difference Vegetation Index (remotely sensed daily values)	Sparse vegetation and seasonality	Vegetation	[-]	(Bohn and Vivoni, 2016)
$NDVI_{min}$	Minimum Normalized Difference Vegetation Index (set to 0.1)	Sparse vegetation	Constant	[-]	(Bohn and Vivoni, 2016)

$NDVI_{max}$	Maximum Normalized Difference Vegetation Index (set to 0.8)	Sparse vegetation	Constant	[-]	(Bohn and Vivoni, 2016)

Table S10. Parameters used for ET estimation in the VIC V4.2 model. Additional information on model parameters was found in the GLDAS project (https://ldas.gsfc.nasa.gov/gldas/GLDASmapveg.php).

[a] PET: potential evapotranspiration equation; Stress: Stress model for actual ET calculation from PET.

S3. Additional information on the determination of parameter ranges

Parameter	Description	unit	Lower limit	Upper limit	Category	Note and references for parameter range
h_{veg}	Vegetation height	[m]	0.2	Site specific	vegetation	The upper bound is set for each site specifically so that it is lower than the measurement heights reported in Table B1.
r_{st}	Stomatal resistance	[s.m^{-1}]	20	600	vegetation	The range includes the 70th percentiles of the values for the different vegetation types in temperate climate (Breuer et al., 2003).
LAI_{min}	Reduction in leaf area index during the dormant season	[%]	5	100	vegetation	Best guess estimate.
LAI_{max}	Annual maximum leaf area index	[m^2.m^{-2}]	0.5	8	vegetation	The range includes the 70th percentiles calculated for the different vegetation types in temperate climate (Breuer et al., 2003).
V_r	Maximum storage capacity of the root zone	[mm]	20	500	vegetation	The range includes the 70th percentiles of the values of rooting depth (provided in [m]) for the different vegetation types in temperate climate (Breuer et al., 2003) multiplied by an average value of soil available water capacity of 0.2 m^{3}m^{-3} (Bonan, 2015; Miralles et al., 2011; Salter and Williams, 1965).
V_{can}	Canopy storage capacity per unit of LAI	[mm LAI]	0.1	0.5	vegetation	The range includes the value used in WaterGap (Döll et al., 2003) for daily application (0.3 mm LAI); in VIC (Liang et al., 1994) and ISBA (Noilhan and Planton, 1989) for subdaily applications as proposed in (Dickinson, 1984) (0.2 mm LAI); in the Distributed Hydrology-Soil-Vegetation model (Wigmosta et al., 1994) for subdaily applications (0.1 mm LAI); the maximum value used in Mac-PDM [Gosling and Arnell, 2011] (0.5 mm LAI for open shrublands).
k	Beer-Lambert's law extinction coefficient	[-]	0.4	0.7	vegetation	The range includes the value reported in (Van Dijk and Bruijnzeel, 2001; Granier et al., 1999; Kergoat, 1998; Ruiz et al., 2010) (0.5); in (Shuttleworth and Wallace, 1985) (0.7).
f_{red}	Reduction factor for transpiration below the root zone	[-]	0	0.15	soil	The range includes the value reported in (Penman, 1950; Wagener et al., 2003) (1/12).
z_0	Soil roughness length	[m]	0.0003	0.013	soil	The range includes the value used in MOSES (Essery et al., 2001) (0.0003m); in Hydrus (Šimůnek et al., 2009) (0.001 m); in NOAH (Yang et al., 2011) and the Community Land model (Oleson et al., 2010) (0.01 m); in (Masson et al., 2003) (0.013 m).
$r_{s,soi}$	Soil surface resistance	[s.m^{-1}]	0	100	soil	The range includes value used in VIC (Bohn and Vivoni, 2016) and SWAP (Kroes et al., 2008) (0 m.s^{-1}); in (Kergoat, 1998) (50 m.s^{-1}); in MacPDM (Smith, 2016) (100 m.s^{-1}); in (Van de Griend and Owe, 1994) (10 m.s^{-1}).
V_e	Maximum storage capacity of the first soil layer	[mm]	5	45	soil	Range includes the average depth of 0.1-0.15 m recommended in (Allen et al., 1998) multiplied by a large value of the soil water capacity of 0.3 m^{3}m^{-3} ((Bonan, 2015; Salter and Williams, 1965)).
a	Spatial variability coefficient	[-]	0	6	soil and epikarst	(Hartmann et al., 2015)
V_{soil}	Mean soil storage capacity	[mm]	20	800	soil	Best guess estimate.
V_{epi}	Mean epikarst storage capacity	[mm]	200	700	epikarst	(Hartmann et al., 2015)
K_{epi}	Mean epikarst outflow coefficient	[d]	0	50	epikarst	(Hartmann et al., 2015)

Table S11. Description of V2Karst parameters, unconstrained ranges used in the application at the four FLUXNET sites to capture the variability across soil, epikarst and vegetation types, category of the parameters (which indicated whether the parameters depend on soil, epikarst or vegetation properties) and references for the determination of parameter ranges. Parameters a, V_{soil}, V_{epi} and K_{epi} were already present in the previous version of the model (VarKarst).

Parameter	Unit	German site (deciduous forest)		Spanish site (shrubland)		French 1 site (evergreen forest)		French 2 site (evergreen forest)		Note and reference for parameter ranges
		Lower limit	Upper limit	Lower limit	Upper limit	Lower limit	Upper limit	Lower limit	Upper limit	
h_{veg}	[m]	23.1	42.9	0.35	0.85	7.1	13.3	3.9	7.2	The range corresponds to the average value reported in Table B1 for the site ±30%. At the Spanish site, the upper bound is set higher due to the presence of a few plants taller than average.
r_{st}	[s.m^{-1}]	275	400	195	350	320	455	320	455	40th and 60th percentile values reported in (Breuer et al., 2003) for the specific land cover at the site.
LAI_{min}	[%]	5	20	34	63	80	100	80	100	At the Spanish site, the range corresponds to the value reported in Table B1 for the site ±30%, and it is a best guess estimates for the other sites.
LAI_{max}	[m^2.m^{-2}]	3.5	6.5	1.9	3.5	1.5	2.9	2.0	3.8	The range corresponds to the value reported in Table B1 for the site ±30%.
V_r	[mm]	60	300	30	200	30	200	30	200	The range includes the average value of the soil available water capacity for the German, Spanish and French 2 sites, and the value of the available water capacity of the root zone for the French 2 site. The upper bound is set to a high value to include uncertainty and to account for the fact that at the German, Spanish and French 1 sites, roots could extend below the soil because the soil is quite shallow.
V_{soi}	[mm]	60	400	30	300	30	300	30	300	Best guess estimates.

Table S12. Site-specific constrained parameter ranges at the four FLUXNET sites for the vegetation parameters (h_{veg}, r_{st}, LAI_{min}, LAI_{max}, V_r) and for the soil storage capacity (V_{soi}) and references for the determination of parameter ranges.

S4. Data processing and analysis at FLUXNET sites

S4.1. Processing of forcing data

Measurements of precipitation, air temperature, net radiation, relative humidity and wind speed were gap-filled and then aggregated from 30 min to daily time scale. Missing precipitation data were filled with zero values for short gaps only (less or equal to 3 h). For all other variables, we used the following procedure for gap-filling:

- short gaps (less of equal to 3h) were filled using linear interpolation;
- medium gaps (from 3.5 h to 15 days) were filled using moving window averaging, i.e. the values for same time of the day for the previous and following days were averaged. For each gap we expanded progressively the width of the moving window until a minimum of four values to calculate the average were found. The maximum width of the moving window was 30 days.
- long gaps (from 15 to 80 days) were filled using long term averaging, i.e. for each month, we derived an average value for each time of the day by calculating the average over the entire time series.

After gap-filling, we could extract for each site a simulation period for which no gap remained.

We then identified the 'poor' months for which the data contained many gaps, and therefore for which the impact of the gap-filling on the simulation results is likely to be significant. 'Poor' months had more than 20 % of the days that contained gap-filled data or were following months in which more than 20 % of the days contained gap-filled data. In fact, after each period of months that contained many gaps, we assumed that the impact of the gap-filling is still significant over a subsequent period containing the same number of months. During such 'poor' months we did not compare model simulations with latent heat and soil moisture observations when applying the soft rules for parameter estimation (Sect. 4.1 of the main paper).

S4.2. Analysis of the uncertainty in observed ET

We analysed the uncertainty in observed ET by calculating the relative difference and the monthly correlation coefficient between the uncorrected actual ET and the Bowen ratio corrected estimates (Eq.(17) of the main paper) and the residual corrected estimates (Eq.(18) of the main paper) at the four FLUXNET sites. Results are reported in Table S13. We observe that the relative difference can be quite large, especially between the uncorrected and the residual corrected estimates, since the relative difference can be as high as 77 %. We see that the Bowen ratio corrected estimate provides an intermediate value, between the uncorrected and the residual corrected estimate. However, the monthly correlation coefficient was always high at all sites (above 0.86), which means that all three estimated have similar temporal dynamics.

Therefore, the magnitude of observed actual ET has large uncertainties at the FLUXNET sites, while the temporal dynamic of observed actual ET seems to be well captured by the measurements.

Site	Relative difference [%]		Monthly correlation coefficient [-]	
	$E_{act,bow}$	$E_{act,res}$	$E_{act,bow}$	$E_{act,res}$
German	16	23	0.97	0.94
Spanish	17	76	0.99	0.87
French 1	10	30	0.97	0.91
French 2	34	77	0.97	0.86

Table S13. Relative difference and correlation coefficient between monthly measured actual evapotranspiration ($E_{act,obs}$) and monthly actual evapotranspiration estimate corrected using the Bowen method ($E_{act,bow}$) or the energy residual method ($E_{act,res}$) at the four FLUXNET sites.

S4.3 Estimation of wind speed at the FLUXNET Spanish for the virtual experiment

To setup the virtual experiment, we transformed the wind speed measurements at the Spanish site to estimate their value at the same height as measured at the German site (43.5 m). In fact, at the Spanish site wind speed is measured at a low height (2.5 m), since the vegetation is short. Therefore, to simulate the impact of a change to tall vegetation (forest) at the shrub virtual site, wind speed should be estimated at a height which is above canopy level, as required by the Penman Monteith equation. We assumed a logarithmic wind profile as e.g. in (Lhomme et al., 2014). We note that we modified Eq. (6) in (Lhomme et al., 2014), which is valid when the vegetation is fully covering the ground, to account for sparse vegetation. We calculated the value of wind speed at 43.5 m over vegetated and non-vegetated fraction separately using Eq. (6) in (Lhomme et al., 2014) and estimated the overall wind speed at 43.5 m for the site as the area weighted value over both fractions. The other climate variables (air temperature and humidity) are assumed to be the same at 43.5 m compared to 2.5 m. We deemed that these assumptions were reasonable, since the objective of the virtual experiment is to understand recharge sensitivity and not to predict future recharge.

S5. Analysis of the impact of the warm-up period for simulations at FLUXNET sites

The analyses reported in this section aim to identify an appropriate value of the warm-up period (denoted as H_w), to evaluate V2Karst at the four FLUXNET sites. The warm-up period corresponds to the initial time period which is discarded to reduce the impact of the choice of the value of the model initial states on the simulations. We assessed the sensitivity of the fluxes simulated with V2Karst to H_w by evaluating the model over a range of values of H_w. For a given FLUXNET site, the date of the first day following the warm-up period is kept constant across the simulations (1 January 2001 at the German site, 1 January 2006 at the Spanish site, 1 January 2010 at the French 1 site and 1 April 2003 at the French 2 site). Instead, the date of the first day of the warm-up period is varied according to the value of H_w. In this way, simulated fluxes are assessed over the same time horizon for all values of H_w and therefore simulations using different values of H_w can be compared among each other. We varied H_w between 2 and 12 months and we assessed the sensitivity of the total simulated recharge (Q_{epi}) and actual ET (E_{act}) to H_w by estimating the metrics ΔQ_{epi} [mm] and ΔE_{act} [mm] defined as follows:

$$\Delta Q_{epi}(H_w = h_w) = Q_{epi}(H_w = h_w) - Q_{epi}(H_w = 12) \qquad (S1)$$
$$\Delta E_{act}(H_w = h_w) = E_{act}(H_w = h_w) - E_{act}(H_w = 12)$$
$$\text{where } h_w = 2, \dots, 11 \ \ months$$

The two metrics of Eq. (S1) measure the difference in Q_{epi} and E_{act} when H_w is set to 12 months compared to when H_w is set to lower values. A large value of ΔQ_{epi} or ΔE_{act} means that the choice of H_w has an impact on simulated recharge and actual ET, while a small value of ΔQ_{epi} or ΔE_{act} means that H_w has little effect on the simulation results. Initially, we assumed that the soil and epikarst stores of V2Karst are saturated. For each of the 11 values of H_w that were tested, we repeated the simulations over 1,000 parameter sets sampled using latin hypercube sampling and the ranges reported in Table 1 of the main paper, and therefore for each site we performed a total number of 11,000 model evaluations.

Figure S1 reports ΔQ_{epi} (left panels) and ΔE_{act} (right panels) against H_w for the 1,000 parameter sets for each FLUXNET site. We see that when H_w increases, the width of the simulation ensemble decreases, which means that the impact of H_w on the simulations decreases. In general, the value of ΔQ_{epi} and ΔE_{act} becomes very small ($-5\ mm < \Delta Q_{epi} < 5mm$ and $-5\ mm < \Delta E_{act} < 5mm$) when H_w is equal to or larger than 10 months, apart from one parameterisation at the Spanish site for which ΔQ_{epi} and ΔE_{act} becomes very small when H_w is equal to 11 months. Therefore, the simulated fluxes show generally little changes in response to changes in H_w when H_w is higher than 10 months.

Consequently, we deemed reasonable to set the warm-up period equal to 12 months at all FLUXNET sites to perform the parameter estimation and the sensitivity analysis presented in this study (Sect. 4.1 and 4.2 in the main paper).

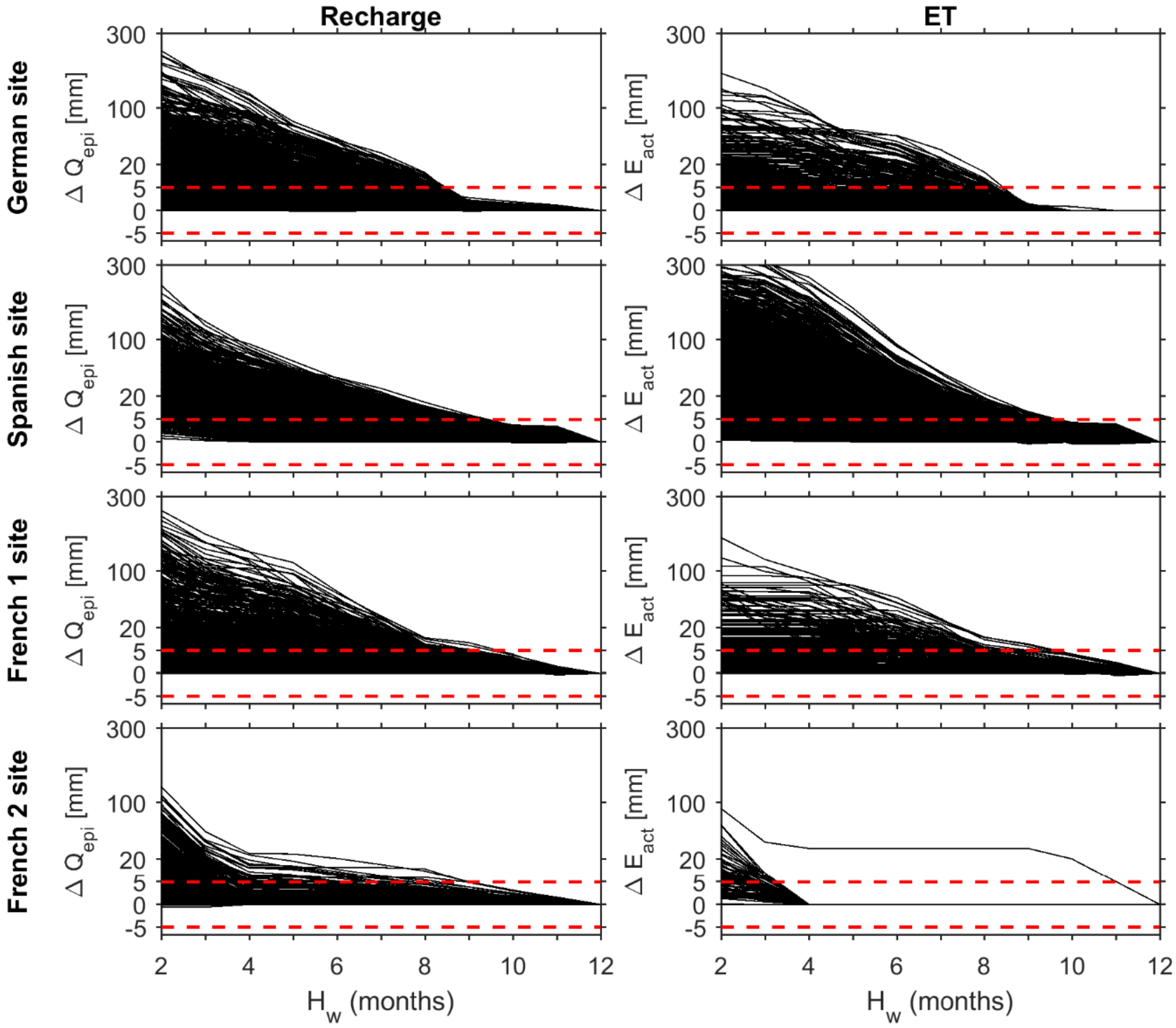

Figure S1. Difference in simulated recharge (ΔQ_{epi}) and actual ET (ΔE_{act}) estimated for varying values of the warm-up period (H_w), and calculated as the difference between recharge (resp. actual ET) simulated when using the value of H_w reported on the x-axis of the plots compared to a value of H_w of 12 months (see Eq. (S1)) at the four FLUXNET sites.

S6. Analysis of range of variation of precipitation characteristics to inform the choice of precipitation inputs for the virtual experiment

This section reports the cumulative distribution function of monthly precipitation P_m $[\mathrm{mm.month}^{-1}]$ (Fig. S2), precipitation intensity I_p $[\mathrm{mm.d}^{-1}]$ (Fig. S3) and interval between wet days H_p [d] (Fig. S4) for:

- the whole domain, which is all European and Mediterranean carbonate rock areas reported in the carbonate rock map of (Williams and Ford, 2006) presented in Fig.1 in the main paper. For this, precipitation from the GLDAS database is used (Rodell et al., 2004);
- the four carbonate rock sites of the FLUXNET network (Baldocchi et al., 2001) analysed in this study and presented in Fig. 1 and Table B1 in the main paper.

These three figures allowed to inform the choice of the ranges of P_m, I_p and H_p to derive the synthetic precipitation inputs used in the virtual experiment (Sect. 4.3 in the main paper).

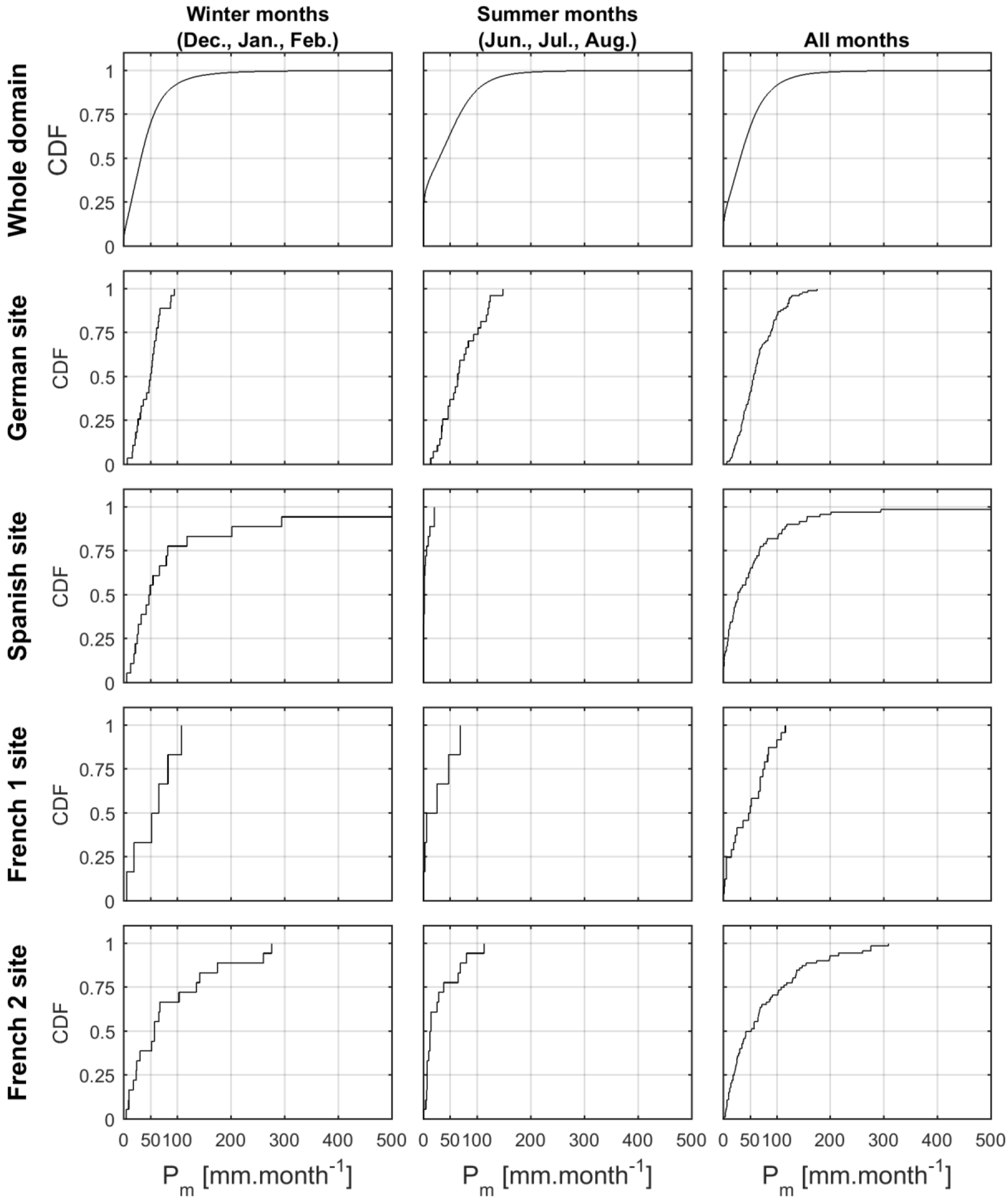

Figure S2. Cumulative distribution function of monthly precipitation P_m [$\mathrm{mm.month^{-1}}$] over winter months (Dec., Jan. Feb.), summer months (Jun., Jul., Aug.) and all months of the year estimated for the whole domain (all European and Mediterranean carbonate rock areas) over the period 1 October 2002–30 September 2012, at the German FLUXNET site over the period 1 January 2001–17 December 2009, at the Spanish FLUXNET site over the period 1 January 2006-30 December 2011, at the French 1 FLUXNET site over the period 1 January 2010–30 December 2011 and at the French 2 FLUXNET site over the period 1 April 2003–31 March 2009.

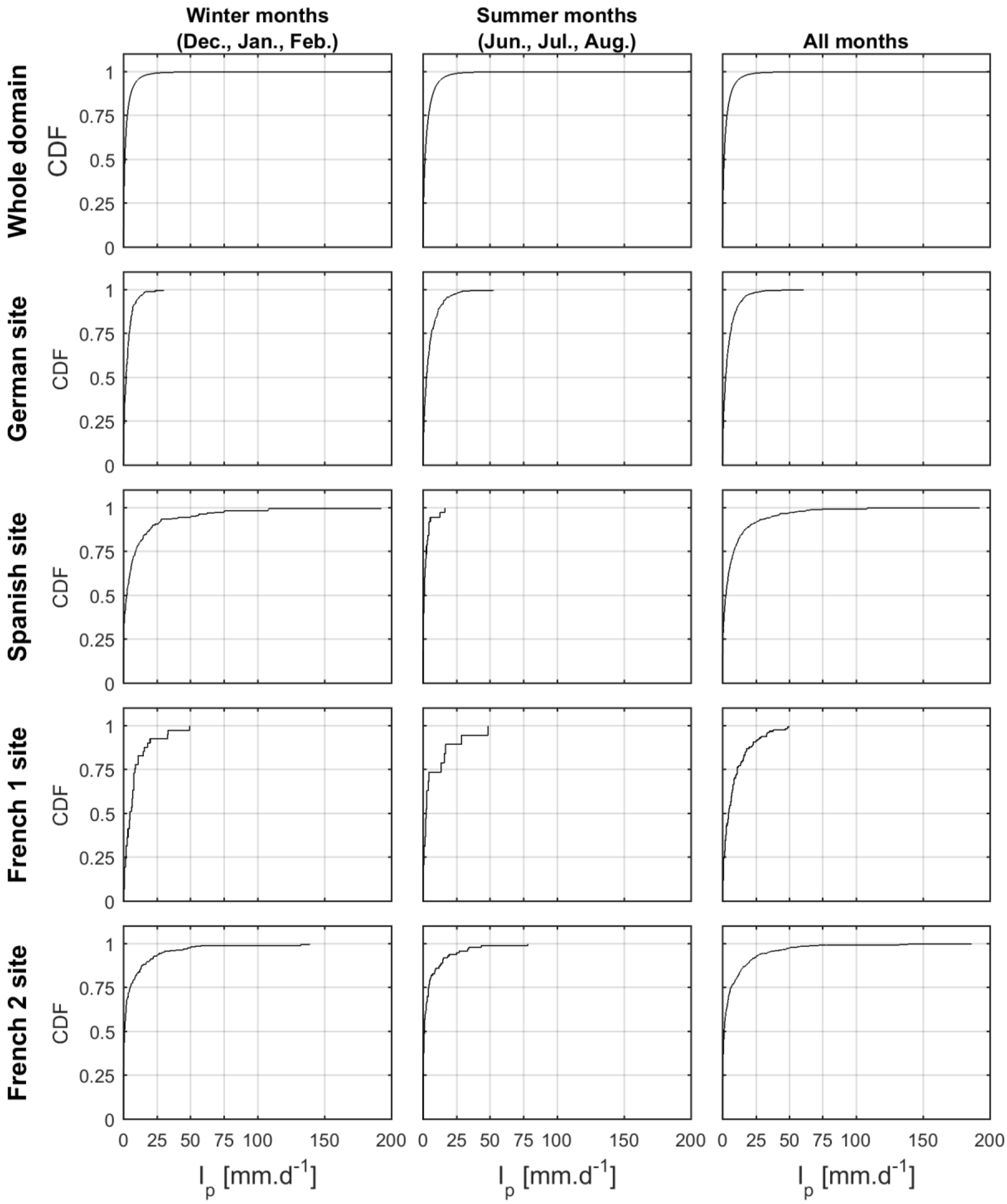

Figure S3. Cumulative distribution function of the precipitation intensity I_p $[\mathrm{mm.\,d^{-1}}]$ over winter months (Dec., Jan. Feb.), summer months (Jun., Jul., Aug.) and all months of the year estimated for the whole domain (all European and Mediterranean carbonate rock areas) over the period 1 October 2002–30 September 2012, at the German FLUXNET site over the period 1 January 2001–17 December 2009, at the Spanish FLUXNET site over the period 1 January 2006-30 December 2011, at the French 1 FLUXNET site over the period 1 January 2010–30 December 2011 and at the French 2 FLUXNET site over the period 1 April 2003–31 March 2009. Only days that had a precipitation amount above 0.1 mm were included in the calculation.

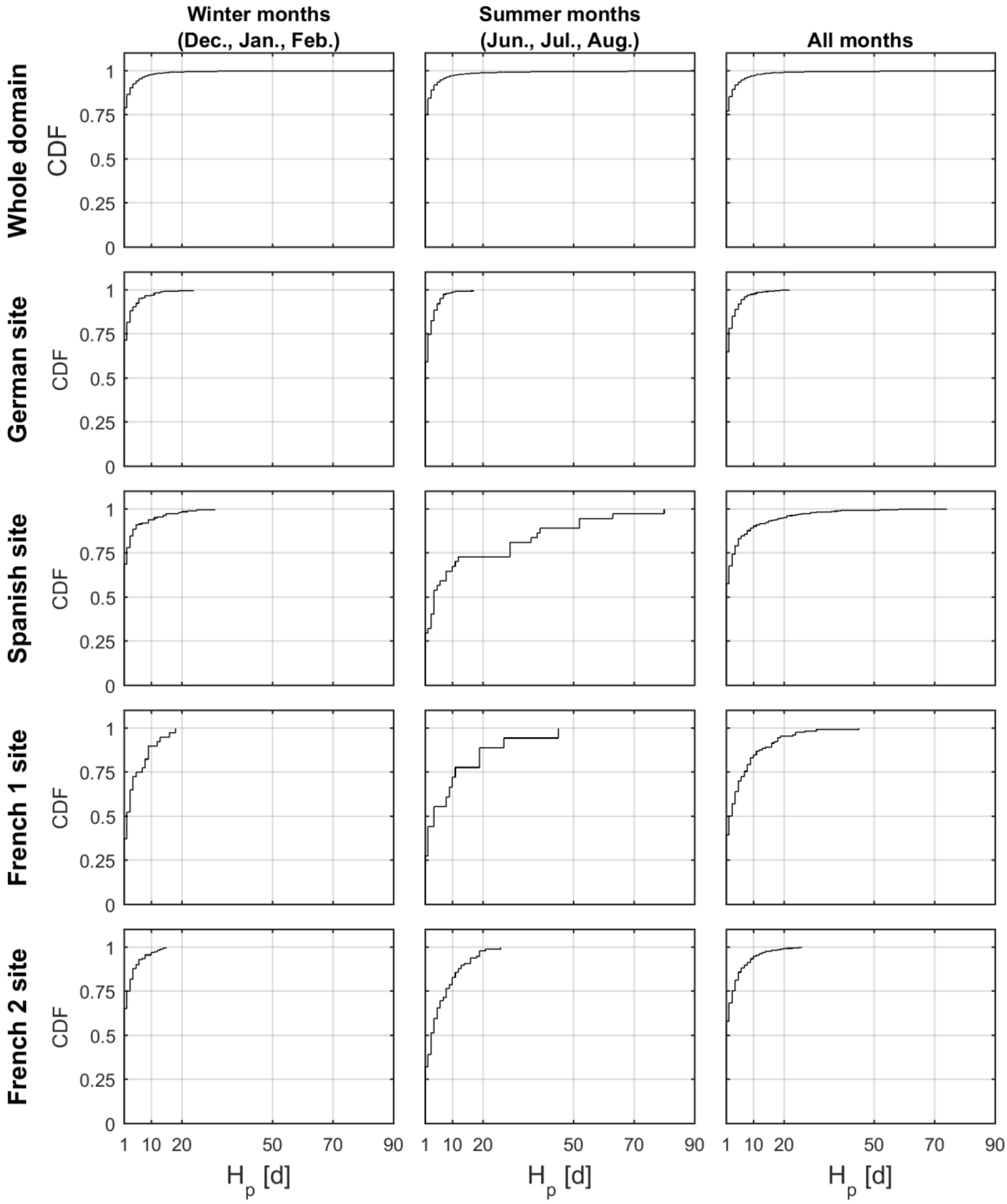

Figure S4. Cumulative distribution function of the interval between wet days H_p $[d]$ over winter months (Dec., Jan. Feb.), summer months (Jun., Jul., Aug.) and all months of the year estimated for the whole domain (all European and Mediterranean carbonate rock areas) over the period 1 October 2002–30 September 2012, at the German FLUXNET site over the period 1 January 2001–17 December 2009, at the Spanish FLUXNET site over the period 1 January 2006-30 December 2011, at the French 1 FLUXNET site over the period 1 January 2010–30 December 2011 and at the French 2 FLUXNET site over the period 1 April 2003–31 March 2009. A wet day is defined as a day with more than 0.1 mm of precipitation.

S7. Sensitivity analysis of V2Karst parameters for the standard deviation of monthly simulated recharge and for simulated actual transpiration

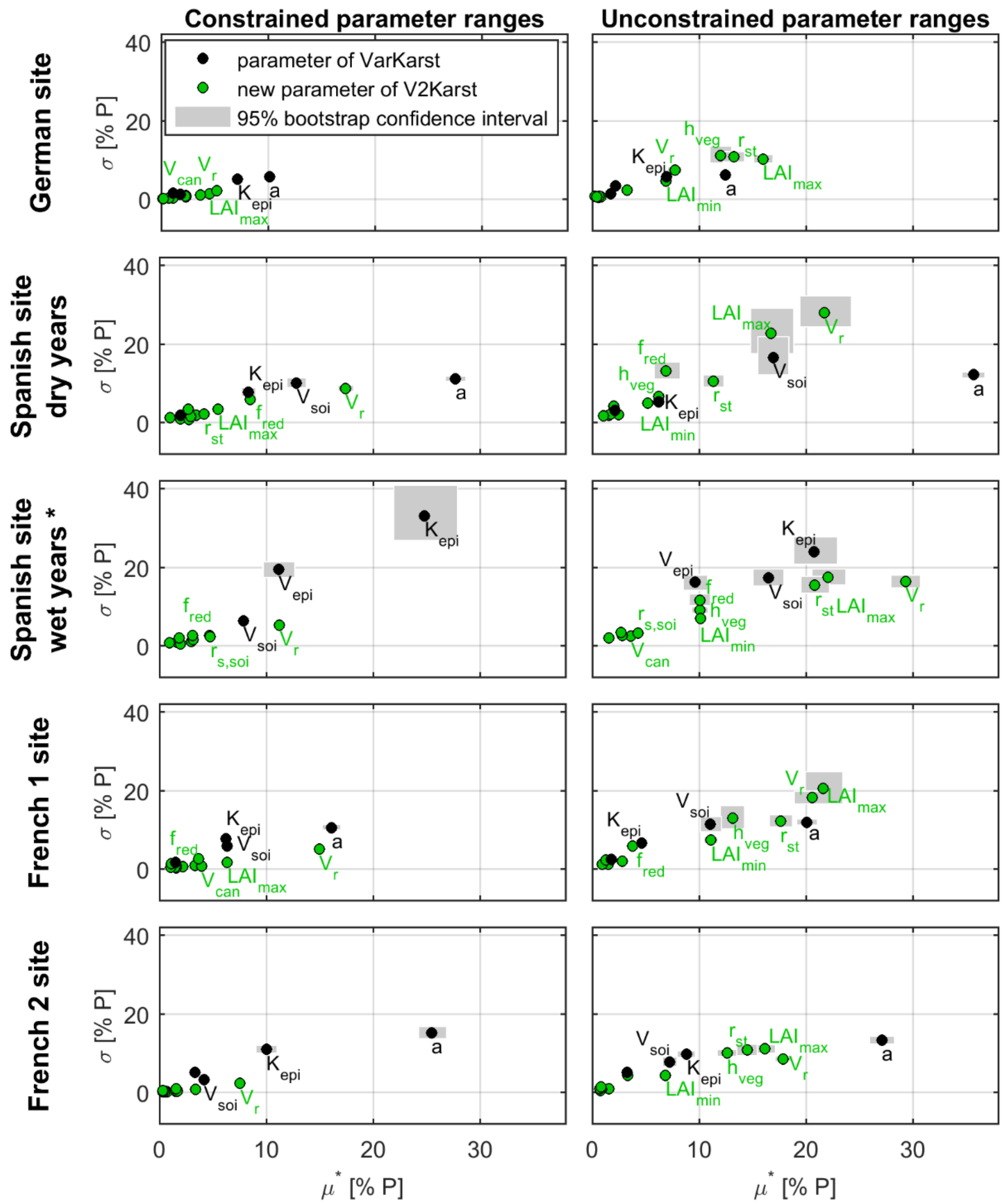

Figure S5. Sensitivity indices of the V2Karst parameters (μ^* is the mean of the absolute Elementary Effects and σ is the standard deviation of the Elementary Effects) for the standard deviation of simulated monthly recharge (expressed as a percentage of mean monthly precipitation) at the four FLUXNET sites when constrained (site-specific) parameter ranges are used (ranges of Table 3 in the main paper) and when unconstrained ranges are used (ranges of Table 1 in the main paper). Sensitivity indices were computed over the period 1 January 2001-17 December 2009 for the German site, 1 January 2006-31 December 2008 for the Spanish site (dry years), 1 January 2009-30 December 2011 for the Spanish site (wet years), 1 January 2010-30 December 2011 for the French 1 site and 1 April 2003-31 March 2009 for the French 2 site.

* Sensitivity indices for parameter a are not reported in the plots for the Spanish site wet years because they are significantly higher than the other parameters ($\mu_a^* = 68\,\%$ and $\sigma_a = 51\,\%$ for constrained ranges and $\mu_a^* = 68\,\%$ and $\sigma_a = 38\,\%$ for unconstrained ranges).

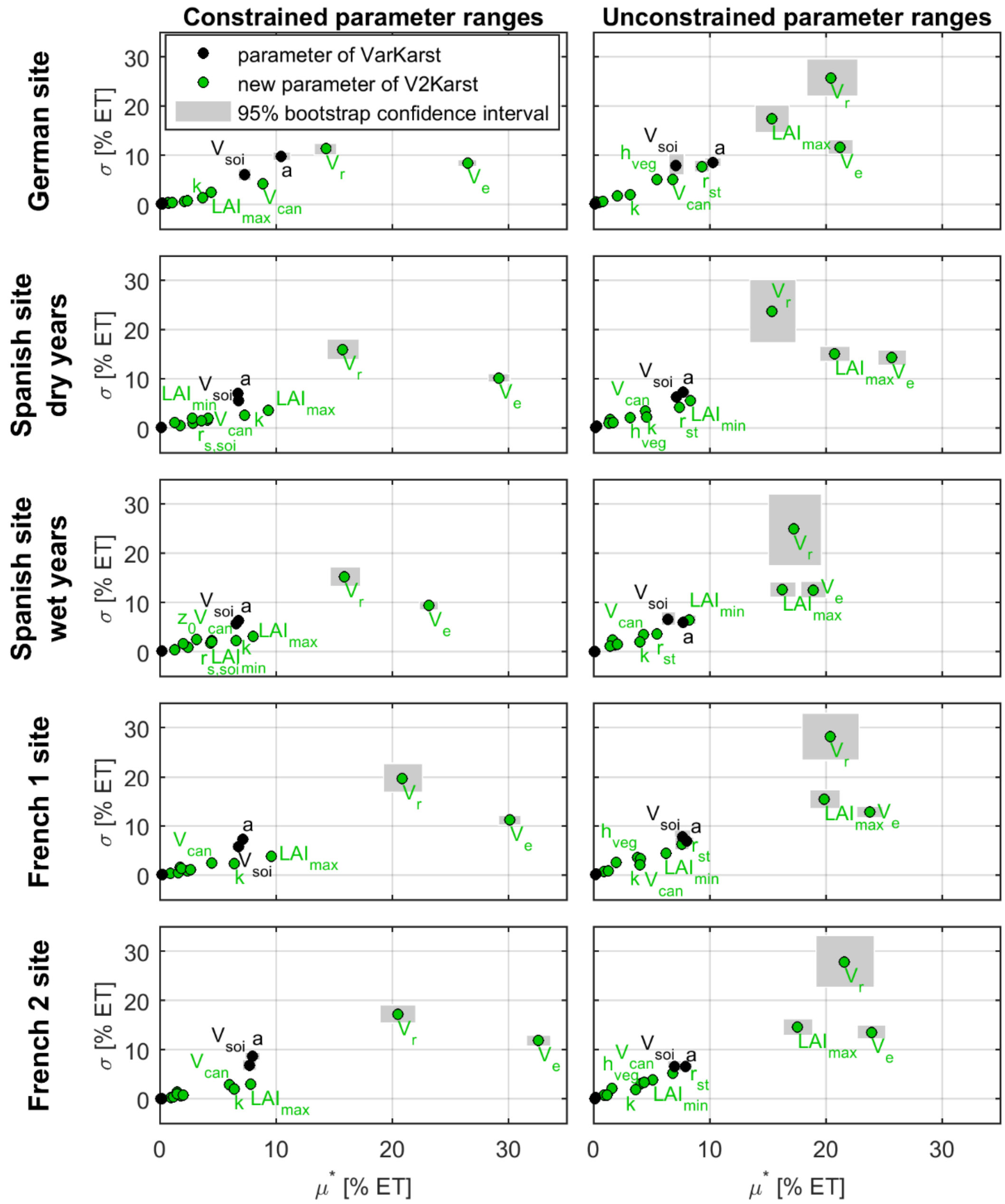

Figure S6. Sensitivity indices of the V2Karst parameters (μ^* is the mean of the absolute Elementary Effects and σ is the standard deviation of the Elementary Effects) for simulated actual transpiration (expressed as a percentage of total ET) at the four FLUXNET sites when constrained (site-specific) parameter ranges are used (ranges of Table 3 in the main paper) and when unconstrained ranges are used (ranges of Table 1 in the main paper). Sensitivity indices were computed over the period 1 January 2001-17 December 2009 for the German site, 1 January 2006-31 December 2008 for the Spanish site (dry years), 1 January 2009-30 December 2011 for the Spanish site (wet years), 1 January 2010-30 December 2011 for the French 1 site and 1 April 2003-31 March 2009 for the French 2 site.

References

Allen, R. G., Pereira, L. S., Raes, D. and Smith, M.: Crop evapotranspiration: Guidelines for computing crop requirements, FAO Irrigation and Drainage Paper 56, Food and Agriculture Organization (FAO), Rome, Italy., 1998.

Arnell, N. W.: A simple water balance model for the simulation of streamflow over a large geographic domain, J. Hydrol., 217(3–4), 314–335, doi:10.1016/S0022-1694(99)00023-2, 1999.

Baldocchi, D., Falge, E., Gu, L., Olson, R., Hollinger, D., Running, S., Anthoni, P., Bernhofer, C., Davis, K., Evans, R., Fuentes, J., Goldstein, A., Katul, G., Law, B., Lee, X., Malhi, Y., Meyers, T., Munger, W., Oechel, W., Paw, K. T., Pilegaard, K., Schmid, H. P., Valentini, R., Verma, S., Vesala, T., Wilson, K. and Wofsy, S.: FLUXNET: A New Tool to Study the Temporal and Spatial Variability of Ecosystem-Scale Carbon Dioxide, Water Vapor, and Energy Flux Densities, Bull. Am. Meteorol. Soc., 82(11), 2415–2434, doi:10.1175/1520-0477(2001)082<2415:FANTTS>2.3.CO;2, 2001.

Baldocchi, D. D. and Ryu, Y.: A Synthesis of Forest Evaporation Fluxes – from Days to Years – as Measured with Eddy Covariance, in Forest Hydrology and Biogeochemistry, Synthesis of Past Research and Future Directions, edited by D. F. Levia, D. Carlyle-Moses, and T. Tanaka, Springer Netherlands, 101–116, Dordrecht., 2011.

Bierkens, M. F. P.: Global hydrology 2015: State, trends, and directions, Water Resour. Res., 51(7), 4923–4947, doi:10.1002/2015WR017173, 2016.

Bohn, T. J. and Vivoni, E. R.: Process-based characterization of evapotranspiration sources over the North American monsoon region, Water Resour. Res., 52(1), 358–384, doi:10.1002/2015WR017934, 2016.

Bonan, G.: Soil Physics, in Ecological Climatology: Concepts and Applications, Cambridge University Press, Cambridge., 143–154, 2015.

Boone, A., Calvet, J.-C. and Noilhan, J.: Inclusion of a third soil layer in a land surface scheme using the force–restore method, J. Appl. Meteorol., 38(11), 1611–1630, doi:10.1175/1520-0450(1999)038<1611:IOATSL>2.0.CO;2, 1999.

Breuer, L., Eckhardt, K. and Frede, H. G.: Plant parameter values for models in temperate climates, Ecol. Modell., 169(2–3), 237–293, doi:10.1016/S0304-3800(03)00274-6, 2003.

Coenders-Gerrits, A. M. J., Van der Ent, R. J., Bogaard, T. A., Wang-Erlandsson, L., Hrachowitz, M. and Savenije, H. H. G.: Uncertainties in transpiration estimates, Nature, 506, E1–E2, doi:10.1038/nature12925, 2014.

Deardorff, J. W.: Efficient prediction of ground surface temperature and moisture, with inclusion of a layer of vegetation, J. Geophys. Res., 83(C4), 1889–1903, doi:10.1029/JC083iC04p01889, 1978.

Dickinson, R. E.: Modeling evapotranspiration for three dimensional global climate models, in Climate Processes and Climate Sensitivity, edited by J. E. Hansen and T. Takahashi, American Geophysical Union, Washington, D. C., 1984.

Döll, P., Kaspar, F. and Lehner, B.: A global hydrological model for deriving water availability indicators: Model tuning and validation, J. Hydrol., 270(1–2), 105–134, doi:10.1016/S0022-1694(02)00283-4, 2003.

Essery, R., Best, M. and Cox, P.: MOSES 2.2 Technical Documentation, Berks, UK. [online] Available from: http://www.metoffice.gov.uk/media/pdf/9/j/HCTN_30.pdf, 2001.

Fang, H., Jiang, C., Li, W., Wei, S., Baret, F., Chen, J. M., Garcia-Haro, J., Liang, S., Liu, R., Myneni, R. B., Pinty, B., Xiao, Z. and Zhu, Z.: Characterization and intercomparison of global moderate resolution leaf area index (LAI) products: Analysis of climatologies and theoretical uncertainties, J. Geophys. Res. Biogeosciences, 118(2), 529–548, doi:10.1002/jgrg.20051, 2013.

Federer, C. A., Vörösmarty, C. and Fekete, B.: Sensitivity of Annual Evaporation to Soil and Root Properties in Two Models of Contrasting Complexity, J. Hydrometeorol., 4(6), 1276–1290, doi:10.1175/1525-7541(2003)004<1276:SOAETS>2.0.CO;2, 2003.

Gerten, D., Schaphoff, S., Haberlandt, U., Lucht, W. and Sitch, S.: Terrestrial vegetation and water balance - Hydrological evaluation of a dynamic global vegetation model, J. Hydrol., 286(1–4), 249–270, doi:10.1016/j.jhydrol.2003.09.029, 2004.

Gosling, S. N. and Arnell, N. W.: Simulating current global river runoff with a global hydrological model: Model revisions, validation, and sensitivity analysis, Hydrol. Process., 25(7), 1129–1145, doi:10.1002/hyp.7727, 2011.

Granier, A., Bréda, N., Biron, P. and Villette, S.: A lumped water balance model to evaluate duration and intensity of drought constraints in forest stands, Ecol. Modell., 116(2–3), 269–283, doi:10.1016/S0304-3800(98)00205-1, 1999.

Hartmann, A., Gleeson, T., Rosolem, R., Pianosi, F., Wada, Y. and Wagener, T.: A large-scale simulation model to assess karstic groundwater recharge over Europe and the Mediterranean, Geosci. Model Dev., 8(6), 1729–1746, doi:10.5194/gmd-8-1729-2015, 2015.

Jung, M., Reichstein, M., Margolis, H. A., Cescatti, A., Richardson, A. D., Arain, M. A., Arneth, A., Bernhofer, C., Bonal, D., Chen, J., Gianelle, D., Gobron, N., Kiely, G., Kutsch, W., Lasslop, G., Law, B. E., Lindroth, A., Merbold, L., Montagnani, L., Moors, E. J., Papale, D., Sottocornola, M., Vaccari, F. and Williams, C.: Global patterns of land-atmosphere fluxes of carbon dioxide, latent heat, and sensible heat derived from eddy covariance, satellite, and meteorological observations, J. Geophys. Res. Biogeosciences, 116(G3), G00J07, doi:10.1029/2010JG001566, 2011.

Kergoat, L.: A model for hydrological equilibrium of leaf area index on a global scale, J. Hydrol., 212–213, 268–286, doi:10.1016/S0022-1694(98)00211-X, 1998.

Körner, C.: Leaf diffusive conductances in the major vegetation types of the globe, in Ecophysiology of photosynthesis, edited by E. D. Schulze and M. M. Caldwell, Springer Study Edition, vol 100, Springer, Berlin, Heidelberg., 463–490, 1995.

Kroes, J. G., van Dam, J. C., Groenendijk, P., Hendriks, A. R. F. and Jacobs, C. M. J.: SWAP version 3.2: Theory description and user manual, Report 1649, Alterra, Wageningen, The Netherlands., 2008.

Lhomme, J. P., Boudhina, N. and Masmoudi, M. M.: Technical Note: On the Matt–Shuttleworth approach to estimate crop water requirements, Hydrol. Earth Syst. Sci., 18(11), 4341–4348, doi:10.5194/hess-18-4341-2014, 2014.

Liang, X., Lettenmaier, D. P., Wood, E. F. and Burges, S. J.: A simple hydrologically based model of land surface water and energy fluxes for general circulation models, J. Geophys. Res., 99(D7), 14415–14428, doi:10.1029/94JD00483, 1994.

Martens, B., Miralles, D. G., Lievens, H., van der Schalie, R., de Jeu, R. A. M., Férnandez-Prieto, D., Beck, H. E., Dorigo, W. A. and Verhoest, N. E. C.: GLEAM v3: satellite-based land evaporation and root-zone soil moisture, Geosci. Model Dev., 10(5), 1903–1925, doi:10.5194/gmd-10-1903-2017, 2017.

Masson, V., Champeaux, J. L., Chauvin, F., Meriguet, C. and Lacaze, R.: A global database of land surface parameters at 1-km resolution in meteorological and climate models, J. Clim., 16(9), 1261–1282, doi:10.1175/1520-0442-16.9.1261, 2003.

McCabe, M. F., Ershadi, A., Jimenez, C., Miralles, D. G., Michel, D. and Wood, E. F.: The GEWEX LandFlux project: Evaluation of model evaporation using tower-based and globally gridded forcing data, Geosci. Model Dev., 9(1), 283–305, doi:10.5194/gmd-9-283-2016, 2016.

Milly, P. C. D. and Shmakin, A. B.: Global Modeling of Land Water and Energy Balances. Part I: The Land Dynamics (LaD) Model, J. Hydrometeorol., 3(3), 283–299, doi:10.1175/1525-754110.1175/1525-7541(2002)003<0283:GMOLWA>2.0.CO;2, 2002.

Miralles, D. G., Gash, J. H., Holmes, T. R. H., De Jeu, R. A. M. and Dolman, A. J.: Global canopy interception from satellite observations, J. Geophys. Res., 115(D16), D16122, doi:10.1029/2009JD013530, 2010.

Miralles, D. G., Holmes, T. R. H., De Jeu, R. A. M., Gash, J. H., Meesters, A. G. C. A. and Dolman, A. J.: Global land-surface evaporation estimated from satellite-based observations, Hydrol. Earth Syst. Sci., 15(2), 453–469, doi:10.5194/hess-15-453-2011, 2011.

Miralles, D. G., Jiménez, C., Jung, M., Michel, D., Ershadi, A., McCabe, M. F., Hirschi, M., Martens, B., Dolman, A. J., Fisher, J. B., Mu, Q., Seneviratne, S. I., Wood, E. F. and Fernaìndez-Prieto, D.: The WACMOS-ET project - Part 2: Evaluation of global terrestrial evaporation data sets, Hydrol. Earth Syst. Sci., 20(2), 823–842, doi:doi.org/10.5194/hess-20-823-2016, 2016.

Müller Schmied, H., Eisner, S., Franz, D., Wattenbach, M., Portmann, F. T., Flörke, M. and Döll, P.: Sensitivity of simulated global-scale freshwater fluxes and storages to input data, hydrological model structure, human water use and calibration, Hydrol. Earth Syst. Sci., 18(9), 3511–3538, doi:10.5194/hess-18-3511-2014, 2014.

New, M., Lister, D., Hulme, M. and Makin, I.: A high-resolution data set of surface climate over global land areas, Clim. Res., 21(1), 1–25, doi:10.3354/cr021001, 2002.

Noilhan, J. and Planton, S.: A Simple Parameterization of Land Surface Processes for Meteorological Models, Mon. Weather Rev., 117(3), 536–549, doi:10.1175/1520-0493(1989)117<0536:ASPOLS>2.0.CO;2, 1989.

Oleson, K. W., Lawrence, D. M., Bonan, G. B., Flanner, M. G., Kluzek, E., Lawrence, P. J., Levis, S., Swenson, S. C., Peter, Thornton, E., Dai, A., Decker, M., Dickinson, R., Feddema, J., Heald, C. L., Hoffman, F., Lamarque, J.-F., Mahowald, N., Niu, G.-Y., Qian, T., Randerson, J., Running, S., Sakaguchi, K., Slater, A., Stöckli, R., Wang, A., Yang, Z.-L., Zeng, X. and Zeng, X.: Technical Description of version 4.0 of the Community Land Model (CLM), NCAR/TN-478+STR, NCAR technical note, National Center for Atmospheric Research (NCAR), Boulder, Colorado., 2010.

Penman, H. L.: The dependance of transpiration on weather and soil conditions, J. Soil Sci., 1(1), 74–89, doi:10.1111/j.1365-2389.1950.tb00720.x, 1950.

Rodell, M., Houser, P. R., Jambor, U., Gottschalck, J., Mitchell, K., Meng, C.-J., Arsenault, K., Cosgrove, B., Radakovich, J., Bosilovich, M., Entin, J. . K., Walker, J. P., Lohmann, D. and Toll, D.: The Global Land Data Assimilation System, Bull. Am. Meteorol. Soc., 85(3), 381–394, doi:10.1175/BAMS-85-3-381, 2004.

Ruiz, L., Varma, M. R. R., Kumar, M. M. S., Sekhar, M., Maréchal, J.-C., Descloitres, M., Riotte, J., Kumar, S., Kumar, C. and Braun, J.-J.: Water balance modelling in a tropical watershed under deciduous forest (Mule Hole, India): Regolith matric storage buffers the groundwater recharge process, J. Hydrol., 380(3–4), 460–472, doi:10.1016/j.jhydrol.2009.11.020, 2010.

Salter, P. J. and Williams, J. B.: The influence of texture on the moisture characteristics of soils- II. Available water capacity and moisture release characteristics, J. Soil Sci., 16(2), 310–317, doi:10.1111/j.1365-2389.1965.tb01442.x, 1965.

Schenk, H. J. and Jackson, R. B.: The Global Biogeography of Roots, Ecol. Monogr., 72(3), 311–328, doi:10.1890/0012-9615(2002)072[0311:TGBOR]2.0.CO;2, 2002.

Shuttleworth, W. J. and Wallace, J. S.: Evaporation From Spare Crops - An Energy Combination Theory, Q. J. R. Meteorol. Soc., 111(469), 839–855, doi:10.1002/qj.49711146910, 1985.

Šimůnek, J., Šejna, M., Saito, H., Sakai, M. and van Genuchten, M. T.: The HYDRUS-1D software package for simulating the one-dimensional movement of water, heat, and multiple solutes in variably-saturated media, Version 4.08, University of California Riverside, Riverside, USA., 2009.

Sitch, S., Smith, B., Prentice, I. C., Arneth, a., Bondeau, a., Cramer, W., Kaplan, J. O., Levis, S., Lucht, W., Sykes, M. T., Thonicke, K. and Venevsky, S.: Evaluation of ecosystem dynamics, plant geography and terrestrial carbon cycling in the LPJ dynamic global vegetation model , Glob. Chang. Biol., 9(2), 161–185, doi:10.1046/j.1365-2486.2003.00569.x, 2003.

Smith, K. A.: Investigating Uncertainty in Global Hydrology Modelling, Ph.D.thesis, University of Nottingham, Nottingham, UK., 2016.

Sperna Weiland, F. C., Vrugt, J. A., Van Beek, R. L. P. H., Weerts, A. H. and Bierkens, M. F. P.: Significant uncertainty in global scale hydrological modeling from precipitation data errors, J. Hydrol., 529(3), 1095–1115, doi:10.1016/j.jhydrol.2015.08.061, 2015.

Sutanto, S. J., Van Den Hurk, B., Dirmeyer, P. A., Seneviratne, S. I., Röckmann, T., Trenberth, K. E., Blyth, E. M., Wenninger, J. and Hoffmann, G.: HESS Opinions "a perspective on isotope versus non-isotope approaches to determine the contribution of transpiration to total evaporation," Hydrol. Earth Syst. Sci., 18(8), 2815–2827, doi:10.5194/hess-18-2815-2014, 2014.

Sutanudjaja, E. H., Van Beek, L. P. H., De Jong, S. M., Van Geer, F. C. and Bierkens, M. F. P.: Large-scale groundwater modeling using global datasets: A test case for the Rhine-Meuse basin, Hydrol. Earth Syst. Sci., 15(9), 2913–2935, doi:10.5194/hess-15-2913-2011, 2011.

Thornthwaite, C. W.: An Approach toward a Rational Classification of Climate, Geogr. Rev., 38(1), 55–94, doi:10.2307/210739, 1948.

Van Beek, L. P. H. and Bierkens, M. F. P.: The Global Hydrological Model PCR-GLOBWB: Conceptualization, Parameterization and Verification, Report Department of Physical Geography, Utrecht University, Netherlands. [online] Available from: http://vanbeek.geo.uu.nl/suppinfo/vanbeekbierkens2009.pdf, 2008.

Van Beek, R.: Forcing PCR-GLOBWB with CRU data, Utrecht University, the Netherlands. [online] Available from: http://vanbeek.geo.uu.nl/suppinfo/vanbeek2008.pdf, 2008.

Van Dijk, A. I. J. M. and Bruijnzeel, L. A.: Modelling rainfall interception by vegetation of variable density using an adapted analytical model. Part 1. Model description, J. Hydrol., 247(3–4), 230–238, doi:10.1016/S0022-1694(01)00392-4, 2001.

Van de Griend, A. A. and Owe, M.: Bare soil surface resistance to evaporation by vapor diffusion under semiarid conditions, Water Resour. Res., 30(2), 181–188, doi:10.1029/93WR02747, 1994.

Vörösmarty, C. J., Moore, B., Grace, A. L., Gildea, M. P., Melillo, J. M., Peterson, B. J., Rastetter, E. B. and Steudler, P. A.: Continental scale models of water balance and fluvial transport: An application to South America, Global Biogeochem. Cycles, 3(3), 241–265, doi:10.1029/GB003i003p00241, 1989.

Vörösmarty, C. J., Willmott, C. J., Choudhury, B. J., Schloss, A. L., Stearns, T. K., Robeson, S. M. and Dorman, T. J.: Analyzing the discharge regime of a large tropical river through remote sensing , ground-based climatic data , and modeling, , 32(10), 3137–3150, doi:10.1029/96WR01333, 1996.

Vörösmarty, C. J., Federer, C. A. and Schloss, A. L.: Potential evapotranspiration functions compared on US watersheds: implications for global-scale water balance and terrestrial ecosystem modeling, J. Hydrol., 207(3–4), 147–169, doi:10.1016/S0022-1694(98)00109-7, 1998.

Wagener, T., McIntyre, N., Lees, M. J., Wheater, H. S. and Gupta, H. V.: Towards reduced uncertainty in conceptual rainfall-runoff modelling: Dynamic identifiability analysis, Hydrol. Process., 17(2), 455–476, doi:10.1002/hyp.1135, 2003.

Wang-Erlandsson, L., Bastiaanssen, W. G. M., Gao, H., Jägermeyr, J., Senay, G. B., Van Dijk, A. I. J. M., Guerschman, J. P., Keys, P. W., Gordon, L. J. and Savenije, H. H. G.: Global root zone storage capacity from satellite-based evaporation, Hydrol. Earth Syst. Sci., 20(4), 1459–1481, doi:10.5194/hess-20-1459-2016, 2016.

Weedon, G. P., Gomes, S., Viterbo, P., Österle, H., Adam, J. C., Bellouin, N., Boucher, O. and Best, M.: The Watch Forcing Data 1958-2001: a Meteorological Forcing Dataset for Land Surface-and Hydrological-Models. Technical Report 22., 2010.

Wigmosta, M. S., Vail, L. W. and Lettenmaier, D. P.: A distributed hydrology-vegetation model for complex terrain, Water Resour. Res., 30(6), 1665–1679, doi:10.1029/94WR00436, 1994.

Williams, P. W. and Ford, D. C.: Global distribution of carbonate rocks, Zeitschrift für Geomorphol. Suppl., 147, 1–2, 2006.

Xue, J. and Su, B.: Significant remote sensing vegetation indices: A review of developments and applications, J. Sensors, 2017, Article ID 1353691, doi:10.1155/2017/1353691, 2017.

Yang, Z.-L., Cai, X., Zhang, G., Tavakoly, A. A., Jin, Q., Meyer, L. H. and Guan, X.: The Community Noah Land Surface Model with Multi-Parameterization Options (Noah-MP) - Technical description, University of Texas at Austin, Austin, USA. [online] Available from: http://www.jsg.utexas.edu/noah-mp/files/noah-mp_technote_v0.2.pdf, 2011.